1989

Bubble sources of the Knudsen sea noise spectra

Medwin, Herman; Beaky, Matthew M.

Acoustical Society of America

Medwin, Herman, and Matthew M. Beaky. "Bubble sources of the Knudsen sea noise spectra." The Journal of the Acoustical Society of America 86.3 (1989): 1124-1130. http://hdl.handle.net/10945/62186

Bubble sources of the Knudsen sea noise spectra

Herman Medwin
Physics Department, Naval Postgraduate School, Monterey, California 93943

Matthew M. Beaky[a)]
Ocean Acoustics Associates, 4021 Sunridge Road, Pebble Beach, California 93953

(Received 5 January 1989; accepted for publication 15 May 1989)

Single coherent bubble contributions to the incoherent underwater noise of spilling breakers have been studied in an anechoic laboratory facility. The waves are generated by a plunger, they propagate 17 m along a 1.2×1.2-m water waveguide, and "spill" and create bubbles at the surface of a $3 \times 3 \times 3$-m anechoic cube of water. Several species of bubbles have been identified. In general, they act as transient dipoles of duration from 2 to several milliseconds, with peak axial source strength of the order of tenths of pascals, at 1 m. The noise is emitted when the bubble is within hundreds of micrometers or a few millimeters of the surface. Bubbles were observed in the 2 decades of frequency from 500 to 50 000 Hz. The average of the individual bubble events yielded a spectrum that slopes at about 5 dB/oct from 1 to 20 kHz, the same as the Knudsen wind noise spectra at sea. The magnitude of the laboratory breaker noise during continual wave-breaking events was approximately 80 dB *re*: 1 μPa^2/Hz at 1 kHz, which is essentially the same as observed during the continual bubble production that occurs with very high winds at sea. The reasons for this agreement are discussed.

PACS numbers: 43.30.Lz, 43.30.Nb

INTRODUCTION

More than four decades ago, Knudsen *et al.*[1] summarized many World War II measurements by characterizing the undersea noise spectrum levels for the frequency range 100 Hz to 25 kHz. Knudsen showed that the levels were wind speed dependent, and that they decrease with increasing frequency at the rate of "about 5 dB per octave." Those "Knudsen curves" were reevaluated and supported by Wenz[2] who added that "air bubbles...could very well be a source of the wind-dependent ambient noise at frequencies between 50 Hz and 10 kHz." Very recently, the NATO-sponsored advanced research workshop on "Sea surface sound" organized by Kerman[3] provided the stimulus for a physical understanding of the phenomenon and its relation to other studies of air–sea interactions. Measurements of the noise of wave breaking in a laboratory flume have been made by Melville,[4] Banner and Cato,[5] and Papanicolaou and Raichlen.[6] Unfortunately, in all these cases the flume was highly reverberant so that absolute noise levels were not obtained. Nor were individual bubble oscillations isolated.

Innovative studies of the noise of breaking waves at sea have been reported by Farmer and Vagle.[7] Shonting and Taylor[8] showed correlations between wind and noise in shallow water.

Recently, Pumphrey and Crum[9] have measured oscillations of bubbles near the surface of a tank of water; the bubbles were created by droplets of water falling onto the surface or by ejection of air from an underwater hypodermic needle. Simultaneous photographic and acoustical measurements have revealed the optical character and the acoustical radiation from these laboratory bubbles.

This past year's theoretical attacks to determine the noise of breaking waves have generally assumed that bubbles are the source of the Knudsen curves. They include Crowther,[10] Hollett and Heitmeyer,[11] Prosperetti,[12] and a highly original series of papers by Longuet-Higgins.[13–15] It is clear that these treatments have been hampered by an inadequate knowledge of several critical inputs to the theories. Unknowns have included the bubble spectrum generated in the wave-breaking process, the character and magnitude of the bubble oscillations and radiation, the duration of the buble oscillations, and the depth of the bubbles when they oscillate. The "bubble spectrum" is defined as the number per unit volume in a 1-μm radius increment; this is generally plotted as a function of bubble radius or resonance frequency.

The observations being reported here are grist for the theorist's mill. We have obtained data from *single* bubbles generated by spilling breakers in a large anechoic tank at the end of a long water tunnel. Since there is no wind, it is clear that these bubbles are more directly correlated with the water surface *slope rather than wind speed*. The bubbles are shown to be mostly shock-excited, very short-duration, transient sources of sound radiating as dipoles at the water surface. Several species of 0.3–50-kHz oscillating bubbles have been identified in terms of the source strength of the dipole sound radiation, the rates of damping, and the constancy of oscillation frequency. The radiated spectral intensities of approximately 100 of these random individual events have been summed incoherently; they produced a frequency spectrum that slopes at approximately 5 dB per octave from 1 to 20 kHz, in general agreement with the Wenz interpretation of the Knudsen wind-related spectra at sea.

[a)] On leave from Physics Department, Worcester Polytechnic Institute, Worcester, MA 01609.

 0001-4966/89/091124-07$00.80

I. EXPERIMENTAL FACILITY

The experiment was conducted in the unique Naval Postgraduate School Ocean Acoustic Wave Facility, OAWF. OAWF consists of a 17-m-long water tunnel (1.2 m wide by 1.2 m deep) terminating in a 3-m-deep anechoic tank, 3 m × 3 m in cross section, which extends 1.8 m below floor level. The tunnel and tank are filled with tap water. The tank bottom and walls are lined with 14-cm-thick absorbing redwood wedges. The last 2 m of the tunnel are lined with 30-cm-long wedges of absorbing "Insulcrete." In the present experiment the breaking waves are produced by an oscillating wedge plunger moving at a frequency of about 1.4 Hz. The "beach," constructed of aluminum shavings in a wedge-shaped nylon net, is quite effective in minimizing wave reflection from the end of the tank (Fig. 1).

The listening system consists of one or two hydrophones of dimension about 6 mm, vertically positioned 12 and 24 cm below the surface of the quiescent water. For the frequencies of this study, the hydrophones and supports are small compared to a wavelength and therefore scatter in the Rayleigh regime. The hydrophones are omnidirectional at frequencies below 50 kHz. They were calibrated by reciprocity, so that the absolute pressure sensitivities are known to better than 1 dB (12%); relative pressures are correct to within 1%.

The signal-analyzing instrumentation is triggered either by a lookout (in some of the early experiments) or by the hydrophone output itself. The background spectral noise levels, and the spectral levels during wave breaking, were determined by use of the calibrated hydrophones and a Hewlett–Packard 3561A dynamic signal analyzer operating at a sampling frequency up to 256 kHz.

The temporal responses of individual bubble radiations are obtained by sending the calibrated hydrophone outputs through an Ithaco 1201 bandpass filter/amplifier to a Computerscope input of an IBM XT. The A/D conversion in this case is at sampling frequency 500 kHz for two channels or 1 MHz for one channel, with 12-bit amplitude resolution. The computer is triggered by the output of the lower hydrophone and can be "backspaced" to determine the signal before triggering.

FIG. 1. Photo of OAWF from the end of the anechoic tank. The horizontal line in the middle of the photo is a breaker over the hydrophones.

II. REVERBERATION, BACKGROUND, AND BREAKER SPECTRA

By using the hydrophones close to the bubble sources, the direct radiation field is very much stronger than the reverberant field, so that the response of a single bubble stands forth quite clearly. To demonstrate this, we measured the elements of reverberation, that is, the multiple echoes from the tank sidewalls and bottom. These were determined by sending impulses of several different frequencies from a 6-mm omnidirectional source, 1 cm under the water surface, to represent a dipole bubble source. Comparison between the direct signal and the echoes and reverberation at the 24-cm hydrophone is shown in Fig. 2. The strongest echo came from the tank bottom at 2 ms; the next strongest generally came from the nearest sidewall, at times less than 2 ms.

For frequencies 5 kHz or higher, the signal-to-reverberant-noise ratio is at least 20 dB. Below 5 kHz the ratio is at worst 15 dB (at frequency 500 Hz) for the hydrophone at 24-cm depth. The hydrophone at 12-cm depth has a signal-to-noise ratio 6 dB better than the data shown in Fig. 2. This test shows that the data reported here are not affected significantly by individual echoes or reverberation in our anechoic tank. These absolute levels can therefore be called "free-field" values.

Long-time averages of the OAWF background noise levels were measured under three conditions: for the facility at rest (room noise); for the plunger in operation, but waves not yet present over the hydrophone; for the plunger in operation at a level such that the waves over the hydrophone were just below breaking amplitude. From 500 to 20 000 Hz the spectral levels of all three conditions were within 0–1.3 dB. The average noise level when waves were not breaking

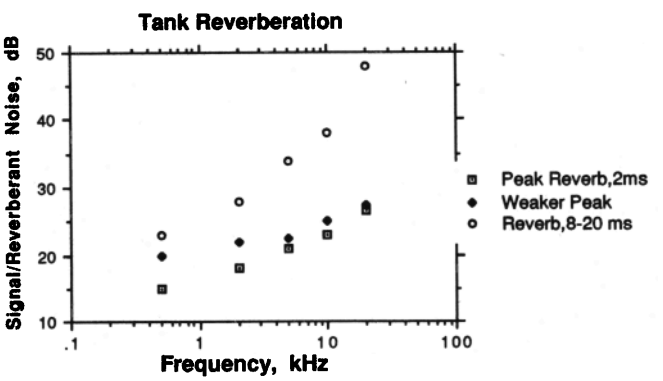

FIG. 2. Signal-to-noise ratio in the reverberation test to the anechoic tank. A source 1 cm under the surface represented bubble radiation. The data were taken from 2 to 20 kHz and extrapolated to 500 Hz.

was less than 1 dB greater than room noise in the tank. The near agreement between the three conditions testifies to the stillness of the vibration-isolated plunger drive system with the 2-m-long anechoic sleeve that was installed at the end of the tunnel, as well as the relative quiet of the wave system before the waves broke.

The dramatic increase in average signal levels, as soon as breakers occur, has been noticed by others as well. In Fig. 3 we show the signal level with breakers measured in two ways: during 150-s continuous operation with intermittent breakers, and during intermittent recording of the noise only when breakers were observed over the hydrophone (to give the impression of continual breaker noise). The room noise spectral levels were subtracted from the signal with breakers to obtain the levels shown in Fig. 3. Both of these spectral slopes of the noise of breakers are approximately 5 dB/octave.

Our purpose in the introductory work described above was to show that we have a quiet, nonreverberant environment for breaker noise measurements, and that our breakers produce noise spectra with a frequency dependence comparable to that obtained during winds at sea (5 dB/octave).

III. CHARACTERISTICS OF THE BUBBLE SOURCES

A. Bubble resonance

We assume that the bubble is spherical, or close enough to spherical, so that, *away from surfaces*, the resonance frequency of the spheroid is given by

$$f_0 = (1/2\pi a)\sqrt{3\gamma P/\rho}, \tag{1}$$

where a = bubble radius, P = ambient pressure at the bubble, ρ = ambient density of the water, and γ = ratio of specific heats of the bubble gas = 1.4. However, for a spherical bubble at close separation z from a free surface, Strasberg[16] showed that the resonance frequency will be higher. For breaker bubbles, which are created at, or very near, the surface, the resonance frequency is given by

$$f = f_0 F, \tag{2}$$

where $F = [1 - (a/2z) - (a/2z)^4]^{-1/2}$, and z = depth.

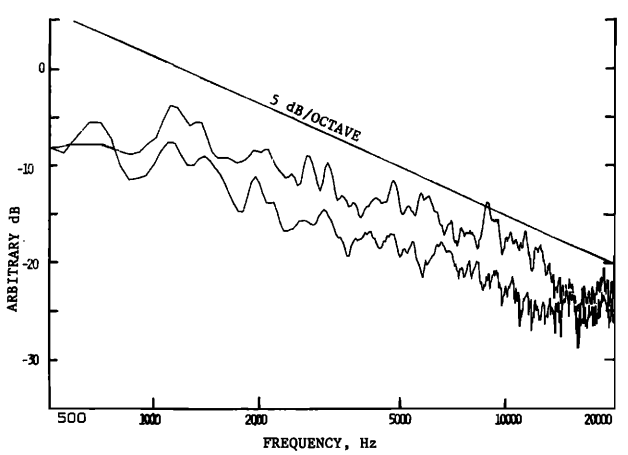

FIG. 3. Breaker noise spectra obtained by two techniques. The lower graph was obtained during continuous recording, the upper graph during intermittent recording when breakers were seen over the hydrophones.

Strasberg[16] also showed that an ellipsoid will have a resonance frequency greater than that of a sphere of the same volume. The frequency becomes closer to the sphere frequency when the eccentricity of the ellipsoid decreases.

B. Bubble damping

Classical bubble theory ascribes exponential damping to acoustic radiation, shear viscosity, and thermal conductivity at the bubble walls[17]; the exponential damping constant is δ. Experimentally, the damping constant is determined by observing the time t_e required for the pressure amplitude to decrease to e^{-1} of its amplitude. The relation is $\delta = (\pi f_0 t_e)^{-1}$.

C. Bubble location

Since the bubbles are produced at the surface and are mirrored in the surface, they act as dipole sources, provided that $kL < 1$, where L is the distance between the bubble and its image (twice the depth of the bubble). Then, the dipole pressure radiated by an oscillating bubble,[18] p_d, is

$$P_d = (k^2/4\pi R)\rho c D \cos\vartheta (1 + i/kR) e^{i(\omega t - kR)}, \tag{3}$$

where ρc = acoustic impedance of water = 1.5×10^6 (mks), $D = VL$ = dipole strength, V = volume/time = $4\pi a^2 U$, U = radial velocity amplitude, ω = angular velocity, R = range from bubble to hydrophone, k = wavenumber, L = distance from bubbler center to image center, kL = nondimensional dipole axis length, and θ = angle between the axis of the dipole and the line joining the source and the hydrophone.

It is often convenient[17] to write this in the farfield version:

$$p_d = p_m (kL \cos\theta), \quad kR \gg 1, \tag{4}$$

where p_m is the magnitude of the farfield monopole pressure. The use of two hydrophones in a line perpendicular to the surface permits one to determine the bubble location (Fig. 4). The complete Eq. (3) is needed because, in our experiment, $0.5 < kR < 20$ and the farfield version does not always apply.

The dipole magnitude is

$$P_d = \frac{k^2 \rho c D \cos\theta}{4\pi R}\left(1 + \frac{1}{k^2 R^2}\right)^{1/2}, \tag{5}$$

and the ratio of the magnitudes measured at corresponding points (e.g., first peak) of the hydrophone outputs is

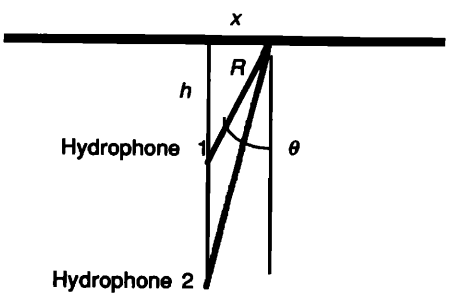

FIG. 4. Geometry for determination of an individual bubble position.

$$\left|\frac{P_{d2}}{P_{d1}}\right| = \frac{h_2}{h_1}\left(\frac{R_1}{R_2}\right)^3\left(\frac{1+(k^2R_2^2)}{1+(k^2R_1^2)}\right)^{1/2}, \quad (6)$$

where h_1 and h_2 are the hydrophone depths and where, because the rms height of our surface is less than 1 cm, we were able to use the approximation $\cos\theta = h/R$ with less than a 2° error in θ.

Considering the phase, we have

$$P_d = |P_d| e^{i(\omega t - kR + \Phi)}, \quad (7)$$

where $\Phi = \tan^{-1}(1/kR)$.

We use peaks which occur at separations $2\pi n$, where n is an integer, so that the time difference between corresponding peaks is

$$t_2 - t_1 = \frac{R_2 - R_1}{c} + \omega^{-1}\left[\tan^{-1}\left(\frac{1}{kR_1}\right) - \tan^{-1}\left(\frac{1}{kR_2}\right)\right]. \quad (8)$$

The geometry is shown in Fig. 4.

Equations (6) and (8), with only R_1 and R_2 being unknown, suffice to determine the ranges and elevation angles to each hydrophone. The azimuthal position is not obtained, but that is irrelevant to the present work: It could be found by using a third hydrophone if needed.

The above analysis assumes that the dipole axis is perpendicular to the horizontal. A third equation relating the ranges and angles is obtained from the geometry in Fig. 4. To determine the actual slope at the bubble dipole location, a sample local tilt of the dipole α is added to, or subtracted from, θ in Eq. (6). The best fit thereby determines α as well. We have found local slopes (of the surface at the dipole) from 0° to 24°.

IV. BUBBLE TYPES

We have looked at over 2000 cases of radiation from individual bubbles, combinations of two or more bubbles, and what we have come to call "nondescript" bubbles occurring when waves break. From this perusal we conducted a census of bubbles and found one type, identified here as type A, (with subclasses A1 and A2) which occurred approximately 65% of the time. A broad overview of several identifiable species and an expanded study of one of the type-A2 bubbles follows.

A. Type A1

Name: Simply damped, spherical bubble.

Description: Impulsive start, constant frequency, single decay rate, experimental damping equal to theoretical damping calculated from radiation, viscosity, and thermal conductivity.[18] First cycle is of shorter duration at lower amplitude compared to second and later cycles.

Physical process: Shock-excited spherical bubble, oscillating at theoretical damping rate, at position more than six bubble radii from the surface ($L/a > 12$). Bubble was ellipsoidal during first cycle.

B. Type A2

Name: Doubly damped, spherical bubble.

Description: Same as type A1, but with an initial damping rate almost twice as great as theoretical; final damping range agrees with theoretical value, e.g., peak pressures on axis at 1 m, 0.35–1.0 Pa; pressure at change of damping rate, 0.10–0.31 Pa. See Figs. 5 and 6.

Physical process: Same as type A1, except that in early stages, bubble is damped, additionally, by a nonlinear dissipation mechanism, perhaps interaction with the ocean surface or generation of acoustic streaming. Several examples of type A2 were sufficiently separated in time, and extended in duration, to permit a detailed evaluation of their characteristics. Case 81-1 is typical (Figs. 5 and 6). The sound frequency was obtained by measuring the peak-to-peak separation times with an accuracy of 2 μs. The frequency was constant 10.4 ± 0.2 kHz (i.e., $\pm 2\%$) for the duration 1300 μs. The initial damping constant (to e^{-1}) was 0.088. The measured final damping constant, 0.053, is in agreement with theory. The initial pressure peak, on the dipole axis referenced to range 1 m, was 0.36 Pa; the pressure at the time when the attenuation changed was 0.13 Pa. The bubble oscillated for 420 μs (approximately four cycles) before it switched to oscillation in the theoretical damping mode.

The diagnosis of this particular bubble radiation can be carried further. It is quite unlikely that the $\pm 2\%$ constancy of the frequency during the observed 1300 μs was caused by a bubble fixed to the surface; a vertical current equal to the orbital velocity of 30 cm/s would have transported the bubble more than one radius and thereby would have lowered its frequency by 35% [calculated from Eq. (2)].

There is a more likely scenario. Since our error in the frequency measurement is less than 4%, and since Eq. (2) predicts a frequency enhancement of less than 4% at a surface separation of $Z > 6a$, it is likely that the bubble was greater than six radii from the surface during the entire 1300 μs while it was transported by turbulence. We believe that it was for *that* reason that the frequency did not change by a perceptible amount. This would mean that $L > 12a$, and $kL > 0.16$, and the effective farfield monopole pressure from which the dipole was formed [see Eq. (4)] was $p_m = p_d/0.16$. That is, the monopole pressure was less than 2.2 Pa at 1 m in this case.

Continuing the linear analysis of this typical type-A

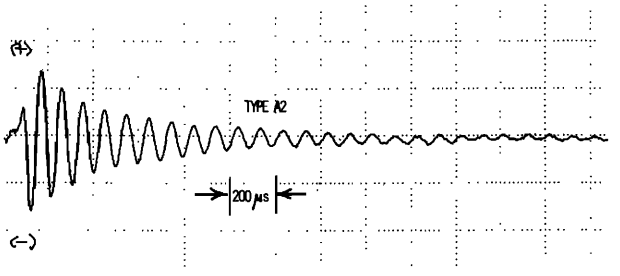

FIG. 5. Acoustic pressure decay for a single type-A resonant at frequency 10.4 kHz (radius 312 μm). Data points at 2-μm intervals. Bubble was at ranges 13.1 and 24.5 cm from the two hydrophones, and at angles 22.2° and 11.5°.

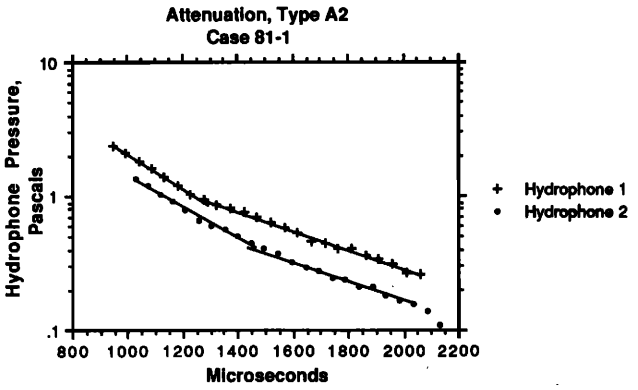

FIG. 6. Two hydrophone data from Fig. 5, replotted to show exponential attenuation rates. The initial slope damping rate is 0.088 (to e^{-1}); final slope is the theoretical value 0.055. Maximum dipole source pressure (1 m, on axis) is 0.36 Pa.

bubble, we know[19] that in the near field of a monopole, at $R = a$, the radial particle velocity is related to the acoustic pressure by

$$u_a = p_a\sqrt{1 + k^2a^2}/(\rho cka), \tag{9}$$

where ρc is the acoustic impedance of the medium. For a resonating bubble in water, because $ka = 0.0136$ and $\rho c = 1.5 \times 10^6$ MKS,

$$u_a = 4.9 \times 10^{-5}\, p_a. \tag{10}$$

For this particular case, on axis at the bubble surface, $R = a = 312\ \mu$m, $u_a < 0.31$ m/s and the displacement amplitude predicted by this linear analysis was $x = (u_a/\omega) < 4.7\ \mu$m. Since this displacement is only about 1.4% of the radius, and since break-up oscillations and bubble shedding have been observed to require a displacement about 8% of the radius,[20] these type-A bubbles are well below break-up instability. That is why type-A2 bubbles show such beautifully clear damped oscillations such as in Fig. 5.

Type-A bubbles are the most common bubbles, by far, having been observed in more than 65% of our studies. Sometimes the double attenuation slopes of type A2 are not clearly identified, and this is probably due to a lower level of excitation. They have been observed over the frequency range 2–30 kHz. These bubbles had dipole source strengths, on axis, ranging from 0.1–1.0 Pa, referenced to 1-m range.

C. Type B

Name: Damped oscillation with spin-off bubbles.

Description: Similar to type A, but intermittently showing highly damped, very much higher frequency radiation. See Fig. 7.

Physical process: Unstable larger bubble, shedding very much smaller bubbles (e.g., a 1-mm bubble spinning off bubbles of radii 65 and 101 μm in Fig. 7).

D. Type C

Name: Near surface, moving bubbles.

Description: Amplitude grows, then decays, accompanied by a change to a much lower frequency. See Fig. 8.

Physical process: Bubble originates at separation much less than six radii from surface. Rapid movement away from near-surface origin, with subsequent increase in amplitude due to an increase in dipole axis L and change of shape from ellipsoidal to spherical form. This is followed by decay due to damping.

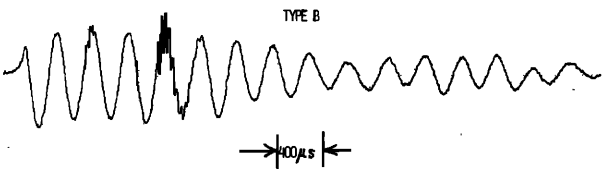

FIG. 7. Case 43-4, type-B bubble. The basic frequency is 3.1 kHz (1.05-mm-radius bubble). The first spin-off bubble is at 50 kHz (radius 65 μm), the second one 32.3 kHz (radius 101 μm). Maximum dipole source pressure (1 m, on axis) is 0.38 Pa.

E. Type D

Name: Amplitude-modulated bubbles.

Description: Pressure amplitude waxes and wanes at a periodicity much less than the bubble resonance frequency. See Fig. 9.

Physical process (Speculative): Two bubbles of slightly different radii have been created, simultaneously, by split up of an ellipsoidal bubble. The two radiations interfere to cause beats.

V. BREAKER SPECTRA AS A SUM OF BUBBLE SPECTRA

If the breaker spectra are simply the sum of the bubble spectra, an incoherent summation of individual bubble intensities would look somewhat like Fig. 3, that is, somewhat like a Knudsen wind noise spectrum with a slope of about 5 dB/octave. A precise proof of this hypothesis would be obtained only after a very large number of individual bubble spectra were obtained for isolated bubble responses. To approach this, we used consecutive spectral windows that were long enough to include the major part of the decay of the longest duration bubbles, 20 ms. Each spectral window then

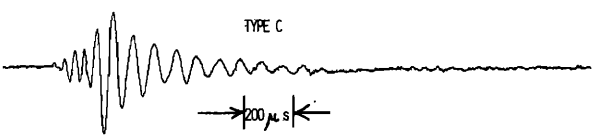

FIG. 8. Case 99-4, type-C bubble. The initial frequency is 25.6 kHz, final frequency 11.5 kHz. Peak pressure 0.33 Pa (1 m, on axis).

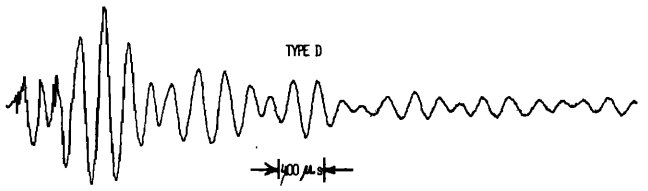

FIG. 9. Case 25-1, type-D bubble. The basic frequency is 4.6 kHz; the amplitude modulation is at approximately 1 kHz with peak pressure 0.9 Pa (at 1 m, on axis).

contained from one to two or three individual bubble spectra because of overlaps.

The prescription was the following: There were five breaking wave events, each containing many bubbles. Each event was split into 20 contiguous blocks, each of duration 20 ms. The Fourier transform was calculated for each block. Then, in order to show the relative power radiated in each band, the sound powers were added for each 50-Hz frequency band. The totals are presented in Fig. 10. The slope is crudely 5 dB/octave from about 1 to 20 kHz, the highest frequency of the Hewlett–Packard spectrum analyzer in this mode.

This graph is noteworthy in that, in addition to the roughly 5 dB per octave slope, several strong peaks are evident at frequencies 1.0, 1.8, 2.6, 3.5, 7.3, and 17.0 kHz. These may be nonlinear, asymmetrical bubble oscillations feeding energy into the breathing mode as predicted by Longuet-Higgins.[15] Those frequencies were predicted to be 1.38, 1.69, 2.10, 2.60, 3.32, 4.31, 5.70, 7.94, 11.4, and 16.8 kHz for modes 15–6, respectively. The partial agreement might be described as "intriguing."

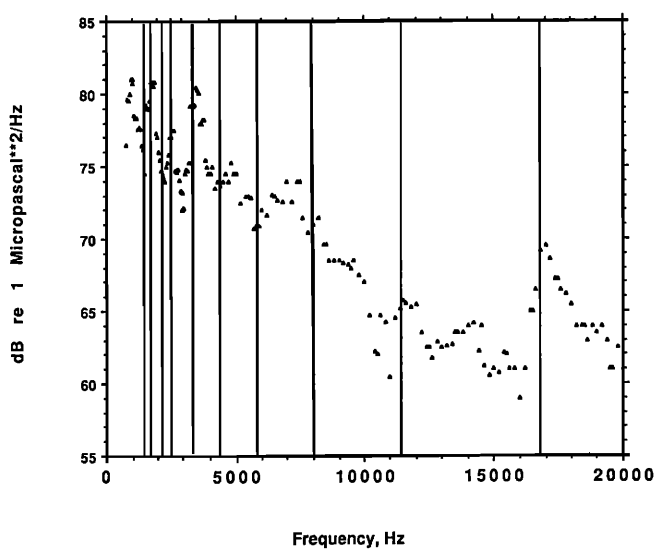

FIG. 10. Sound power spectrum obtained by adding the powers in 400-, and 50-Hz bands for 100 20-ms blocks of spectral energy during five breaking events. Hydrophone depth 24 cm. The vertical lines are the Longuet-Higgins predictions. The decreased spectral levels at $f < 1$ kHz may have been caused by insufficient integration time for these low-frequency bubbles.

Figure 10 is noteworthy, also, in that these absolute levels measured at 24-cm depth in a freshwater laboratory tank are almost the same as measured at great depths under violent storms at sea. This startling observation is discussed below.

VI. CONCLUDING COMMENTS

There is a long history of ocean noise being "instantly" sensitive to the onset of winds. Since waveheight depends on the fetch and duration of the wind, it is not the waveheight that is crucial to ocean noise; it is the presence of breaking waves. This was clearly evident in these laboratory experiments.

We have presented laboratory-acquired evidence that, when a wave spills (even without wind), the catastrophically created bubbles are transient sources of underwater noise only during the several milliseconds of their early lives. The spectral slope in the no-wind laboratory resembles the Knudsen wind wave spectra at sea. The implication is that the ocean noise in the frequency range 1–20 kHz, and perhaps at higher and lower frequencies as well, is due to wind only through the mediation of the spilling breakers which are the sources of the sound-radiating bubbles.

One notes that independence of depth exists when the noise sources are uniformly distributed over the surface that is being sensed. This is so because, although the farfield intensity from a single source varies with depth as h^{-2}, the area of the surface, and the number of sources sensed in a receiving beam pattern, varies with depth as h^2. Of course, this independence of average noise level on depth is modified by attenuation due to scatter and absorption. And it is modified in shallow water or when the receiver is close to the bottom. Furthermore, the dependence of bubble formation on the salinity, temperature, and organic content must be considered for a complete comparison of laboratory and ocean.

By listening to the surface only at times, and under regions, when there were noise-generating spilling breakers, we obtained levels as great as those found in deep ocean measurements during violent storms when almost all of the sensed surface was active. We believe that the magnitude of the breaker noise level depends on the fraction of the sensed surface over which spilling breakers are generating noise at the instant of the noise measurement (in retarded time). Sea surface noise does not depend on the number of senile bubbles that may be seen as a froth from above or counted from below the surface.

ACKNOWLEDGMENTS

Valuable discussions have been held with L. A. Crum, D. M. Farmer, M. S. Longuet-Higgins, W. K. Melville, J. A. Nystuen, and F. Raichlen. Additional measurements were made by Lt. Albert C. Daniel, Jr., U.S.N. The support of the Office of Naval Research has made this research possible.

[1]V. O. Knudsen, R. S. Alford, and J. W. Emling, J. Marine Res. 7, 410–429 (1948).
[2]G. M. Wenz, J. Acoust. Soc. Am. 34, 1936–1956 (1962).
[3]B. R. Kerman, Ed., *Sea Surface Sound* (Kluwer Academic, Dordrecht,

The Netherlands, 1988).
[4]W. K. Melville and R. J. Rapp, pp. 39–50 in Ref. 3.
[5]M. L. Banner and D. H. Cato, pp. 429–436 in Ref. 3.
[6]P. Papanicolaou and F. Raichlen, pp. 97–110 in Ref. 3.
[7]D. M. Farmer and S. Vagle, pp. 403–416 in Ref. 3.
[8]D. Shonting and N. Taylor, pp. 417–428 in Ref. 3.
[9]H. C. Pumphrey and L. A. Crum, pp. 463–484 in Ref. 3.
[10]P. A. Crowther, pp. 131–150 in Ref. 3.
[11]R. D. Hollett and R. M. Heitmeyer, pp. 449–462 in Ref. 3.
[12]A. Prosperetti, pp. 151–172 in Ref. 3.
[13]M. S. Longuet-Higgins, J. Fluid Mech. **201**, 525–541 (1989).
[14]M. S. Longuet-Higgins, J. Fluid Mech. **201**, 543–565 (1989).
[15]M. S. Longuet-Higgins, "Bubble noise spectra," J. Acoust. Soc. Am. (submitted).
[16]M. Strasberg, J. Acoust. Soc. Am. **25**, 536–537 (1953).
[17]C. S. Clay and H. Medwin, *Acoustical Oceanography* (Wiley, New York, 1977); Chap. 6, Sec. A5.1.2.
[18]P. M. Morse and K. U. Ingard, *Theoretical Acoustics* (McGraw-Hill, New York, 1968), p. 312.
[19]L. E. Kinsler, A. R. Frey, A. B. Coppens, and J. V. Sanders, *Fundamentals of Acoustics* (Wiley, New York, 1982), 3rd ed.
[20]D. L. Storm, "Interfacial distortions of a pulsating gas bubble," in *Finite-Amplitude Wave Effects in Fluids*, edited by L. Bjørno (IPC Science and Technology, Guildford, Surrey, England, 1974).